Electrochemical Behavior of Fe$_3$Al Modified with Ni in Hank´s Solution

C.D Arrieta-Gonzalez[1,2], J. Porcayo-Calderon[3,], V.M. Salinas-Bravo[3], J.G. Gonzalez-Rodriguez[4], J.G. Chacon-Nava[1]*

[1] Centro de Investigación en Materiales Avanzados, Miguel de Cervantes 120, 31109-Chihuahua, Chihuahua, MEXICO.
[2] Instituto Tecnológico de Zacatepec, Depto. De Ingeniería Química y Bioquímica, Av. Instituto Tecnológico 27, Zacatepec, Morelos, MEXICO
[3] Instituto de Investigaciones Eléctricas, Gerencia de Materiales y Procesos Químicos, Av. Reforma 113, Col. Palmira, 62490-Cuernavaca, Morelos, MEXICO.
[4] Centro de Investigación en Ingeniería y Ciencias Aplicadas-UAEM, Av. Universidad 1001, Col. Chamilpa, 62210-Cuernavaca, Morelos, MEXICO.
[*] E-mail: jporcayo@iie.org.mx

An investigation about the corrosion resistance of Fe$_3$Al-type intermetallic alloys in Hank´s solution was carried out via electrochemical techniques. The Fe$_3$Al intermetallic alloy was modified with additions of Ni and evaluated in the as cast and thermal treated conditions. For comparison, Titanium and 316-L stainless steel were also evaluated. For evaluation purposes, electrochemical techniques included potentiodynamic polarization curves, open circuit potential measurements, linear polarization resistance curves and cyclic polarization curves were employed. Results shown that the 316-L stainless steel and titanium are the materials with greater corrosion resistance in chloride-rich environments showing an active-passive behavior and are susceptible to pitting corrosion. Compared to 316-L SS and Titanium, intermetallic Fe$_3$Al alloys had greater susceptibility to pitting corrosion. Ni addition changed the corrosion potential of the intermetallic base Fe$_3$Al to more noble values. Ni addition and thermal treatment improved the corrosion resistance of Fe$_3$Al-base alloy owing to an increased stability of the passive layer.

Keywords: intermetallics, corrosion, Fe$_3$Al, chlorides, biomaterials

1. INTRODUCTION

Biomaterials are materials used in the manufacture of devices that interact with biological systems and coexist for a long period of service with minimal failure. They are widely used for repairing or replacement of components of the tissue-skeletal system such as bones, joints and teeth.

[1].

The fundamental requirement of a biomaterial is that material and body tissue environment can coexist without any undesirable or inappropriate effect on each other. Biocompatibility is an essential requirement for any biomaterial. Medical devices made from biomaterials are hip replacements, heart valves, neurological prostheses and systems for drug delivery. Devices placed inside the body for a defined time are known as implants, and those placed permanently as a prosthesis [2].

Orthopedic implants have improved the quality of life for millions of people. The clinical goal is to relieve pain and increase ease of movement in joints. The engineering goal is to provide the minimum physiological strain. Integrity and functionality of bone and prosthetic materials has to be maintained for a period of long service. Suitable materials for implants are those tolerated by the body and they should be able to withstand cyclic loading in the aggressive environment of the body [3].

The fundamental criterion of a biomaterial is its biocompatibility. Metals and alloys have been widely used as implants and they provide the mechanical strength and corrosion resistance required. Metallic implants are generally made of one of these three types of materials: austenitic stainless steel, chromium-cobalt alloys, and titanium and its alloys [3].

In particular, the 316-L stainless steel is used as an implant material because of a favorable combination of mechanical properties, corrosion resistance, biocompatibility satisfactory and relatively low cost compared to other biomaterials such as titanium. Body fluids are considered as a corrosive environment due to its high Cl^- concentration and temperatures of 36.7-37.2°C. This makes a favorable environment for the phenomenon of pitting corrosion on 316-L stainless steel, with a consequent release of metal ions of Fe, Cr and especially Ni, which can cause toxicity and impair the biocompatibility of the stainless steel [4]

Pitting manifests as a breakdown of the passive film at local areas giving raise to the formation of microgalvanic cells in which the anode area is represented by pits and the cathode is the large surrounding impervious passive surface. Generally, the evaluation of pitting corrosion resistance of materials is done by accelerated testing methods for identifying the characteristic pitting potential. The pitting nucleation potential, Enp is defined as the lowest potential from which pits nucleate and grow on a passive surface. The pitting protection potential, Epp is the potential below which pitting, once grown, cannot further propagate and hence repassivate. At potentials between Enp and Epp, pittings can grow but new pits cannot nucleate [5].

Although iron aluminides have been investigated primarily for high temperature structural applications due to its ability to form a protective layer of Al_2O_3 that provides corrosion resistance in molten salt environments [6, 7], its excellent performance in these conditions has motivated its study in aqueous solutions. The use of iron aluminides is being considered for applications at room temperature to replace stainless steels. Considering that, Fe_3Al alloys do not contain strategic elements such as Cr and Ni; so, these materials are also bear in mind for applications as biomaterials [8].

Thus, the proposal of this work is to investigate the effect of Ni content in Fe_3Al alloy on its corrosion resistance in human body solutions for potentially biomaterials applications. Evaluation of intermetallic alloys were done in as cast and thermally treated conditions. In addition, Ti and 316-L stainless steel were also investigated to compare the performance of the intermetallic alloys.

2. EXPERIMENTAL PROCEDURE

2.1 Materials

Fe$_3$Al intermetallic alloys were cast in an induction furnace and pure Ni was added in quantities of 1, 3 and 5% (by weight). The elements used were of purity greater than 99.9%. To evaluate the effect of intermetallic alloys in as cast and thermal treatment conditions, some castings were thermally treated at 400°C for 120 hours in an electric muffle under argon atmosphere. Specimens made from commercial titanium and 316-L stainless steel were prepared. Table 1 shows chemical composition of materials tested in this investigation.

Table 1. Different metallic materials tested

Material	Type	Chemical composition (wt.%)
Stainless steel	AISI 316L	18 Cr, 12 Ni, 2.5 Mo, <0.03 C, and balance iron
Titanium	Commercial purity	99.6 %
Intermetallic	Fe$_3$Al	12.86 Al, 87.14 Fe
	Fe$_3$Al-1Ni	12.5 Al, 1.03 Ni, balance iron
	Fe$_3$Al-3Ni	12.12 Al, 3.15 Ni, balance iron
	Fe$_3$Al-5Ni	11.7 Al, 5.02 Ni, balance iron

2.2 Sample Preparation

The first step for sample preparation is to cut the alloys into useful samples. Samples were cut down to 5.0 x 5.0 x 3.0 squares using a diamond tipped blade. Sample surfaces were ground down using silicon carbide sandpaper. Grinding process began with 120-grit sandpaper until all major scratches and burs were removed.

The process was continued with 220, 400, and 600-grit sandpaper until all surfaces were uniform. Once the grinding was complete, samples were washed with distilled water then by ethanol in an ultrasonic bath for 10 minutes before the tests.

2.3 Electrochemical techniques

Corrosion behavior of biomaterials can be studied in either vivo or in vitro using artificial physiological fluids at 37°C, in which the oxygen content is controlled at a suitably low value. Hank's solution is an example of an artificial solution, which has been used for corrosion testing in the laboratory.

In this study, the corrosion resistance of different materials were tested by using various electrochemical techniques in de-aerated Hank's solution of pH 7.4 (Table 2). This solution simulate body fluid environment, at 37°C (98.4°F), which is equivalent to human body temperature. Temperature control of Hank´s solution was maintained in the limit of ± 1°C.

Table 2. The composition of Hank´s solution

Compound	Composition [g/l]
NaCl	8.0
$CaCl_2$	0.14
KCl	0.40
$NaHCO_3$	0.35
Glucose	1.00
NaH_2PO_4	0.10
$MgCl_2.6H_2O$	0.10
$Na_2HPO_4.2H_2O$	0.06
$MgSO_4.7H_2O$	0.06

Electrochemical experiments were performed using an ACM Instrument controlled by a personal computer. A typical three electrode arrangement was used with a saturated calomel reference electrode and a platinum wire was the auxiliary counter electrode. The volume of solution in the cell was 100 ml. Nitrogen gas was used for de-aeration of the electrolyte.

Corrosion rates were obtained by potentiodynamic curves polarizing the specimens from -300 to 600 mV with respect to the corrosion potential, E_{corr}, at a scanning rate of 60 mV/min. To assess the ability of the different materials to form a protective oxide scale on their surfaces upon immersion in the simulated body fluid environment free corrosion potential as a function of time of the working electrodes E_{corr}, was measured versus a saturated calomel reference electrode (SCE). Linear polarization curves were obtained by polarizing the specimens from -30 to 30 mV with respect to the free corrosion potential value, E_{corr}, at a scanning rate of 10 mV/min and corrosion current density values, i_{corr}, were calculated. A cyclic polarization technique was used to evaluate pitting and crevice corrosion resistance of the different materials according to the ASTM F2129-01 and ASTM G3-89 or ASTM G61-86. The working electrode was stabilized at the free corrosion potential for an hour, and then it is applied a sweep (0.166 mV/s) in the anodic direction until the potential reaches a predetermined value. At this point, the scan direction is reversed until the hysteresis loop closes. At the point where the current increases sharply is known as the potential of pitting nucleation, Enp, and when the current is zero (during the reverse sweep) are called the protection potential, Epp.

Surface analysis of corroded samples was performed in a Karl Zeiss DSM-950 scanning electron microscope (SEM).

3. RESULTS AND DISCUSSION

3.1 Potentiodynamic Polarization Curves

Samples were immersed in the electrolyte and potential was measured. Potentiodynamic polarization test was started until corrosion potential reached a stable value (after approximately 60 minutes). Figures 1 and 2 show the potentiodynamic polarization curves for different materials tested.
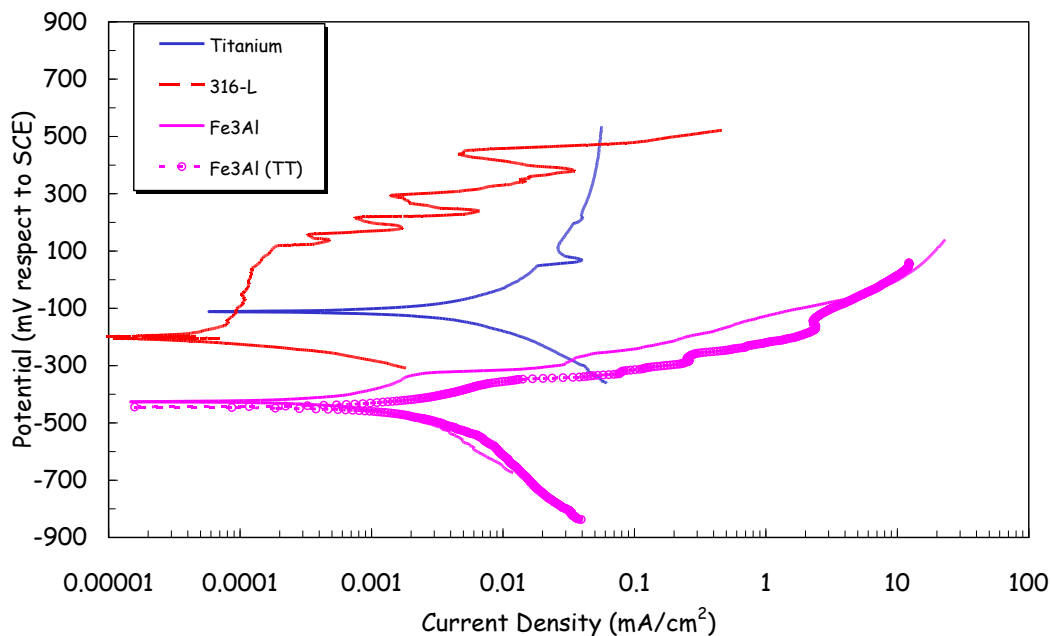
Figure 1. Potentiodynamic polarization plots of Ti, 316-L, Fe₃Al and Fe₃Al(TT) in de-aerated Hank´s solution at 37°.
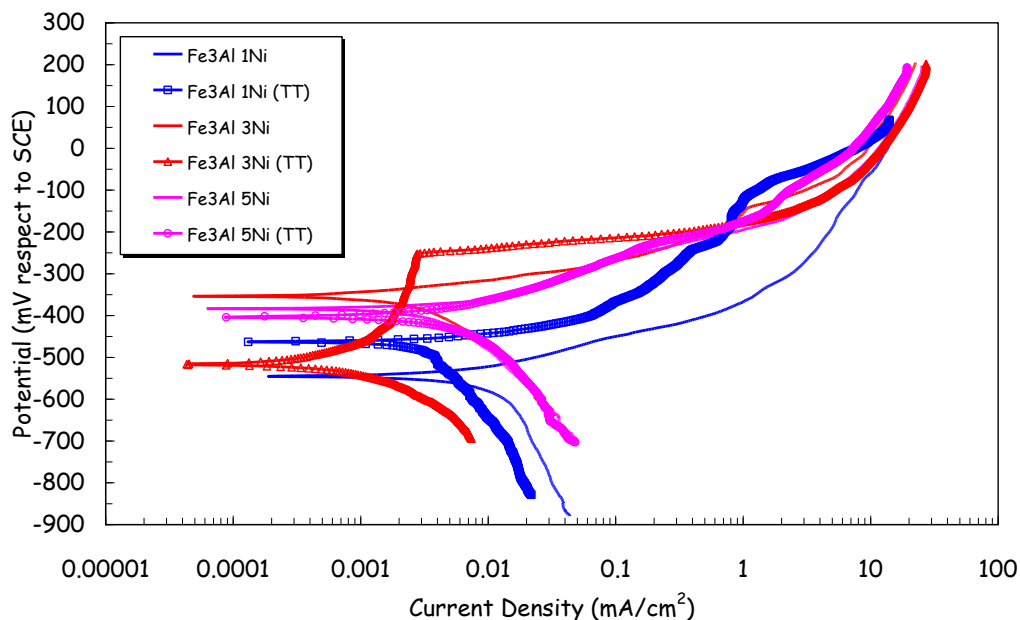

Figure 2. Potentiodynamic polarization plots of Fe₃Al modified with Ni in as cast and thermally treated in de-aerated Hank´s solution at 37°.

From curves in Figure 1 and 2, it was determined the corrosion potential and corrosion current densities. Table 3 summarizes these values. It can be seen that both Ti and 316-L stainless steel were the materials with more noble corrosion potential.

Table 3. Electrochemical parameters of potentiodynamic polarization tests.

Materials	E_{corr} (mV)	i_{corr} (mA/cm^2)
Titanium	-111	0.0045
316-L	-198	0.00007
Fe$_3$Al	-426	0.00095
Fe$_3$Al-1Ni	-545	0.0065
Fe$_3$Al-3Ni	-354	0.002
Fe$_3$Al-5Ni	-383	0.0028
Fe$_3$Al (TT)	-444	0.0015
Fe$_3$Al-1Ni (TT)	-462	0.0033
Fe$_3$Al-3Ni (TT)	-515	0.0004
Fe$_3$Al-5Ni (TT)	-404	0.0003

In the case of Ti, it can be observed a uniform corrosion process with a decrease in the current density, about 100 mV above the corrosion potential. Increasing potential to more noble values, there is a slight tendency to passivate, showing a breakdown and regeneration process of the passive layer; probably generating TiO$_2$ as has been reported in other studies [9-11].

It was observed that 316-L stainless steel showed the lowest corrosion current density, hence the lowest corrosion rate of all materials tested. From the polarization curve, it was observed the formation of a passive zone, with a constant breakdown of the passive layer, possibly due to pitting corrosion process as was observed by SEM [12].

Polarization curves for as casting Fe$_3$Al intermetallic alloy, show more active corrosion potentials compared to Ti and 316-L. This indicates a greater susceptibility to corrosion. At more positive potential a sharp increase in the current density is observed, indicating pitting attack. The morphology of pits is similar to that reported by other authors for pitting attack of intermetallic alloys in environments containing chlorides [8].

In the as cast condition, addition of 1% Ni did not show a definite trend in the corrosion potential behavior. In particular, the addition of 1% Ni decreased the corrosion potential of the Fe$_3$Al intermetallic base. However, additions of 3% Ni and 5% Ni increased the corrosion potential to more noble values. Current density values of Fe$_3$Al with Ni additions are of the same order of magnitude, but higher than those of Ti and 316-L. According to other studies [13], it is expected that the thermal treatment of the intermetallic alloys improves its ductility and change its corrosion behavior. Additions of 1% Ni and 3% Ni to the thermal treated intermetallic Fe$_3$Al alloy changed the corrosion potential to more active values, but addition of 5% Ni raised it to more noble values. Corrosion current density values of the thermal treated Fe$_3$Al and Fe$_3$Al + 1% Ni alloys were of the same order of magnitude. However, Fe$_3$Al with additions of 2 and 3% Ni are one order of magnitude smaller.

3.2 Free Corrosion Potential Curves

Determination of the chemical interaction of metallic materials/bone prothesis with the body fluid environment is essential in order to understand their stability in the human body. One simple way to study the film formation and passivation of implants/alloys in a solution is to monitor the E_{corr} as a function of time. A rise of potential in the positive direction indicates the formation of a passive film, and a steady potential indicates that the film remains intact and protective. A drop of potential in the negative direction indicates breaks in the film, dissolution of the film, or no film formation [14]. E_{corr} as a function of time for different materials tested in the present investigation is presented in Figure 3.

Figure 3. E_{corr} values as function of testing time for the different materials in de-aerated Hank´s solution at 37°.

According to these concepts, it can be seen that Ti shows an active-passive behavior. In the first 25 hours shows an active behavior and then shows a tendency to passivate due to the formation of a protective layer on its surface. This material is the one that showed the more stable trend. Likewise, 316-L stainless steel showed a similar trend as Titanium, however, at 70 hours it showed a sharp drop in E_{corr} and then a passive behavior. This abrupt drop in E_{corr} may be due to the susceptibility of this material to pitting corrosion in chloride-rich environments.

Fe$_3$Al intermetallics in the as cast and thermally treated conditions, showed higher active potentials and fluctuating trends in E_{corr} values. This behavior is consistent with other studies that have shown the pitting corrosion susceptibility of such materials [15] confirmed from the SEM observations.

Ni additions to the Fe$_3$Al intermetallic alloys, modified their behavior making them more noble. However, the E_{corr} trend was similar to the alloy-base in as cast and thermally treated conditions.

In the case of as cast Fe$_3$Al-1%Ni, the trend was more active at the end of the test; on the other hand, the thermally treated condition was more passive. In the case of as cast Fe$_3$Al-3%Ni, it becomes more passive at the end of the test and more active in the thermal treatment condition. Fe$_3$Al-5%Ni behavior was similar to that shown by Fe$_3$Al-1%Ni. In general we can say that Ni addition did not improve the pitting corrosion resistance of Fe$_3$Al according to SEM observations.

3.3 Linear Polarization Curves

Figures 4 and 5 show the evolution of the i$_{corr}$ obtained by linear polarization measurements over time of different materials tested. According to Figure 4, Ti exhibited the smallest i$_{corr}$ values. This indicates the high corrosion resistance of this material in chlorides-rich environments, due to their ability to form a passive layer with high pitting corrosion resistance.

Figure 6 shows the surface aspect of Ti after the polarization test. There was a clean surface free of visible pitting and little accumulation of corrosion products. These observations are consistent with those reported in other studies [9-11] where it is indicated that the corrosion resistance of Ti in chloride-rich environments occurs because of the development of a passive layer of TiO$_2$.

According to i$_{corr}$ measurements shown in Figure 4, 316-L stainless steel also showed a good performance. A higher corrosion resistance was observed in the first 70 hours and then i$_{corr}$ showed fluctuations until the end of the test. This performance is consistent with E$_{corr}$ measurements shown in Figure 3, where an active–passive condition is observed because of constant breakdown and regeneration of the passive layer. Observations by SEM showed a clean surface without accumulation of corrosion products and the presence of small pits along the direction of the surface finish (figure 7).
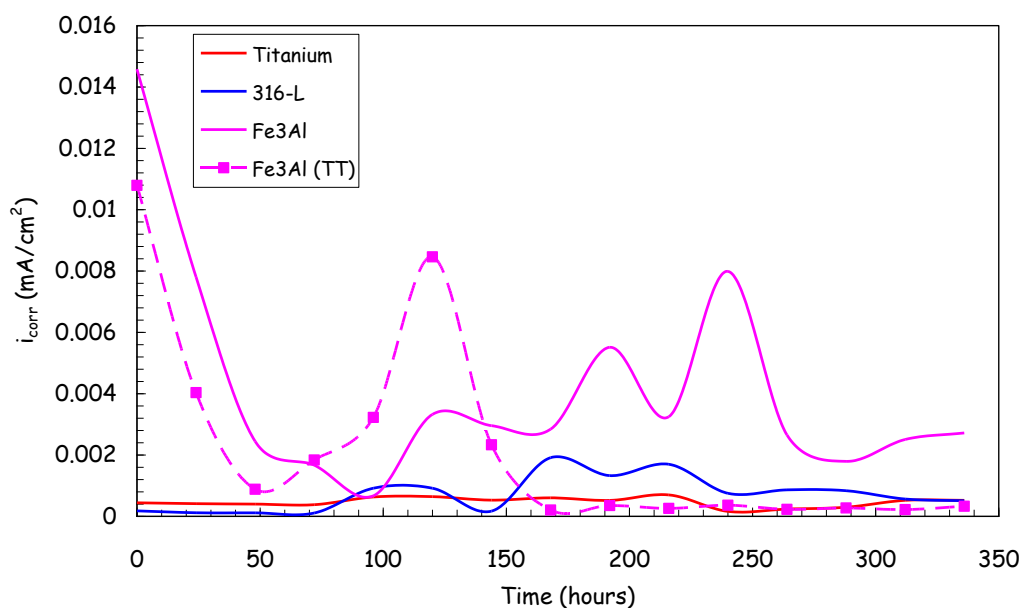

Figure 4. Current density (i$_{corr}$) plots of Ti, 316-L, Fe$_3$Al as cast and Fe$_3$Al(TT) in de-aerated Hank´s solution at 37°.

Fe$_3$Al intermetallic alloys, in as cast and thermally treated conditions, showed a decrease in i$_{corr}$ values the first 50 hours, then exhibit random behavior. This may be due to the attempt of the material to form a passive layer on its surface and then be attacked by the chloride-rich environment without being able to regenerate its passive layer. Fe$_3$Al thermally treated showed an apparent passivity after 170 hours of immersion, but observing its surface after the corrosion test, it showed the accumulation of large amounts of corrosion products. These prevented free access of Cl ions to its surface and limited the attack; contrasting with the same material in as cast condition as shown in the micrographs in Figure 8. This figure shows the highest pitting density in the as cast Fe$_3$Al, and lower accumulation of corrosion products that allowed free access of Cl ions. On the contrary, in Fe$_3$Al thermally treated, there is less pitting density but deeper pits. The passive layer formed on the Fe$_3$Al in as cast thermally treated conditions, was not able to protect it in chlorides-rich environments [15]
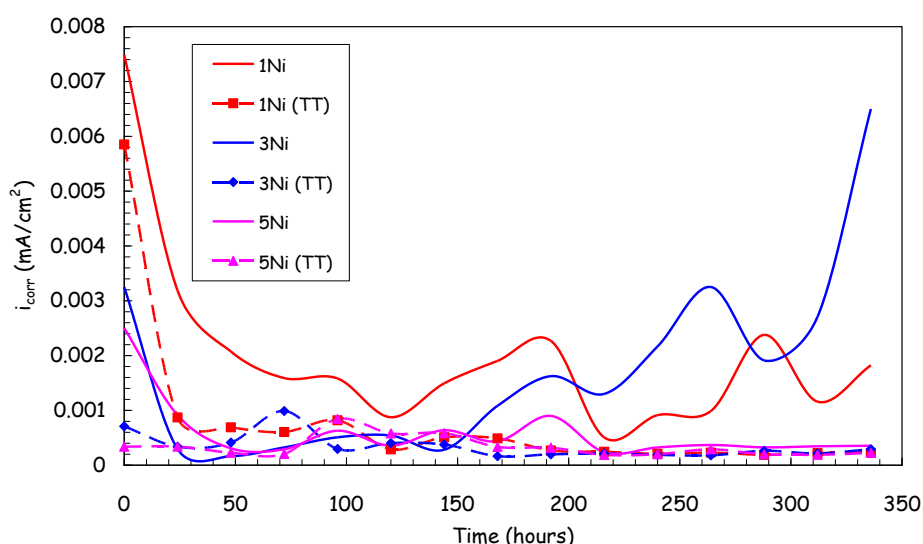

Figure 5. Current density (i$_{corr}$) plots of Fe$_3$Al modified with Ni in as cast and thermally treated in de-aerated Hank´s solution at 37°.
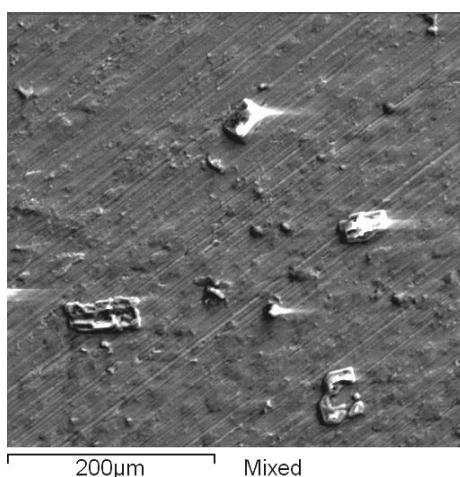

Figure 6. SEM photographs of Ti after corrosion studies in de-aerated Hank's solution at 37°C.
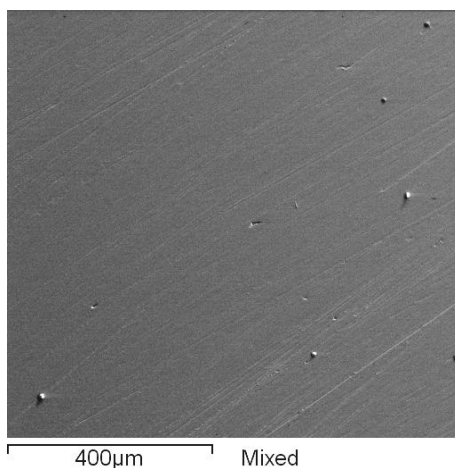
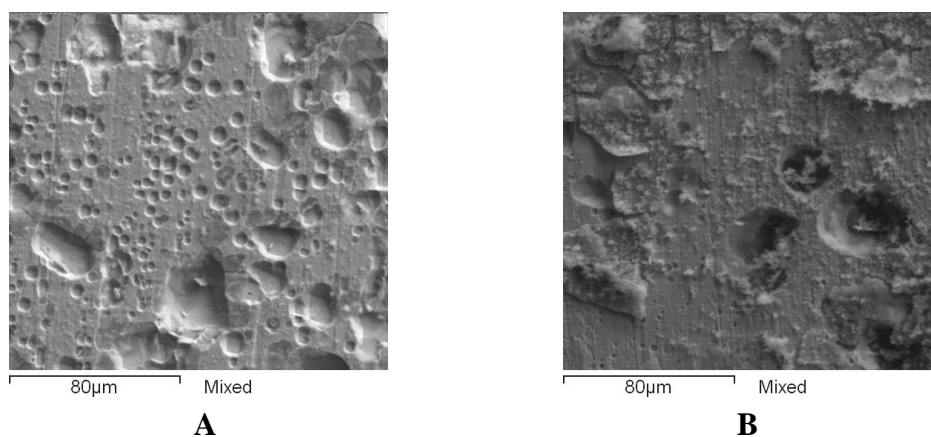**Figure 7.** SEM photographs of 316-L after corrosion studies in de-aerated Hank's solution at 37°C.

Figure 8. SEM photographs of Fe$_3$Al (a) as cast and (b) thermally treated after corrosion studies in de-aerated Hank's solution at 37°C.

Ni addition to Fe$_3$Al increased its corrosion resistance according to the i$_{corr}$ values observed in Figure 5. However, their performance depends on the amount of Ni added and the initial state of the material, i.e. as cast and thermally treated conditions. In general, the i$_{corr}$ values decreased with increased Ni content and thermal treatment conditions. All thermally treated materials showed the lowest i$_{corr}$ values. Ni addition seems to increase the stability and corrosion resistance of the passive layer towards the action of Cl ions; however, does not inhibit pitting attack as observed in the surface analysis performed.

Figure 9 shows the different superficial aspects of Fe$_3$Al intermetallic alloys modified with Ni in the as cast and thermally treated conditions. In all cases, a passive layer on the alloys surface was produced, but it was not stable enough because it was attacked by the Cl ions and caused pitting attack in different extent depending on the Ni content.

In case of the Fe$_3$Al-1Ni alloy, it was observed that in as cast condition, the passive layer was broken and favored the pitting attack in unprotected areas. Detachment of the passive layer was not

observed in thermally treated condition; however, attack and nucleation of larger pits encourage rupture points in the passive layer.

The addition of 3%Ni allowed a greater stability of the passive layer; however, the presence of imperfections in the passive layer allowed diffusion of Cl ions that caused pitting attack. In the thermal treatment condition many imperfections in the passive layer were observed, which resulted in a higher pitting density but smaller in size.

Fe3Al-5Ni in as cast and thermally treated conditions showed a more stable passive layer and lower accumulation of corrosion products (Figure 9). Few pits were observed in the as cast condition, however, in the heat treated condition pits are smaller and have a low density distribution. These tests show that addition of 5%Ni to Fe_3Al increased significantly his corrosion resistance and that the thermal treatment further enhances its performance because of a better alloy homogenization.
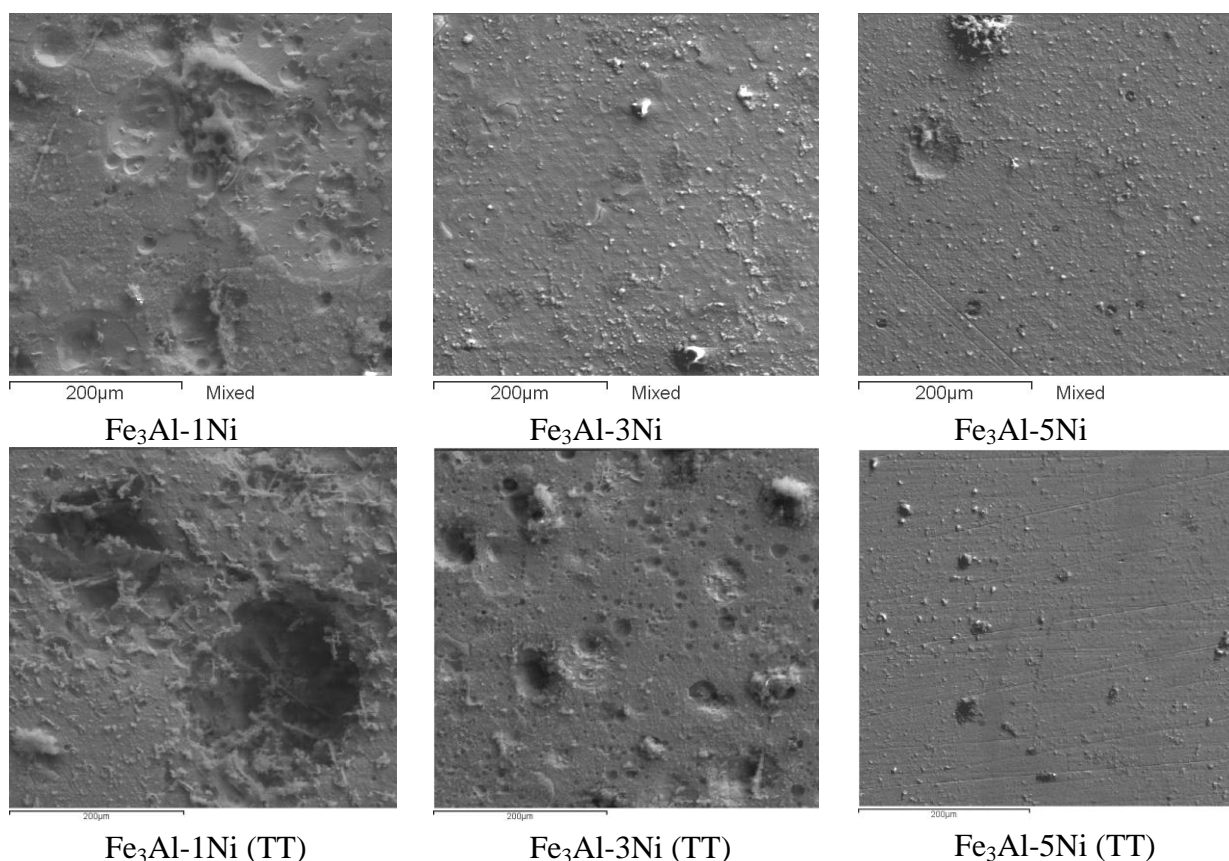

Figure 9. SEM photographs of Fe_3Al modified with Ni in the as cast and thermally treated conditions after corrosion studies in de-aerated Hank's solution at 37°C.

3.4 Cyclic Polarization Curves

Any material or alloy proposed for use as a biomaterial must exhibit excellent resistance to pitting and crevice corrosion, and this characteristic was determined by cyclic polarization tests. Figure

10 shows the cyclic polarization curves for Ti, 316-L and Fe$_3$Al in as cast and thermally treated condition.

Ti shows a largest passive zone than that shown by the 316-L, i$_{corr}$ values of both materials are the same order of magnitude. Ti has the noblest pitting nucleation potential and repassivation potential of all alloys tested: 880 mV and 725 mV respectively. In the interval of 580 and 880 mV light disturbances are observed. As reported by other studies [9-11], these disturbances are produced because of the breakdown and regeneration of the TiO$_2$ passive layer formed.

The range of stability of the passive zone depends on the scan rate used in the cyclic polarization tests. In other studies carried out in similar conditions to this study, it is reported that the passive zone of Ti is about 2000 mV [16] or 3000 mV [17] with respect to their corrosion potential. The significant difference of these works is the use of a scanning rate of 6 mV/min and 4 mV/min respectively, compared to 10 mV/min used in this study.

The excellence of titanium as biomaterial it is due to the passive layer that forms on its surface which protects it from electrochemical attack in the human body. This layer is composed of amorphous titanium oxides from Ti$_2$O to TiO$_2$, having variable thickness between 0.5 and 10 nm according to the treatment, surface finish, corrosive medium, etc. [18-20]. It is reported that the passivation layer is formed naturally after a few milliseconds of contact with a medium with oxygen, but also can be produced and become thicker by chemical and electrochemical treatments [21]. Surface observations showed no visible presence of pits after the polarization test (figure 11).

316-L showed low values of current density with a pitting nucleation potential of 530 mV and a protection potential of 134 mV, both with regard to the corrosion potential. Inside its passive zone the presence of a metastable pitting region is observed. H. Yang et.al. [4] obtained similar results as those reported here under the same experimental conditions, except that in their work they reported a pitting potential of 233 mV.
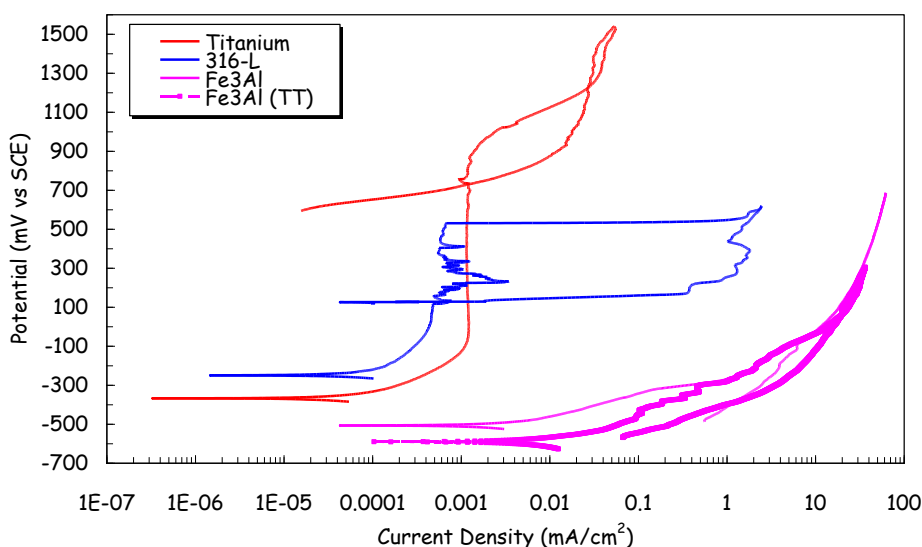

Figura 10. Cyclic polarization plots of Ti, 316-L, Fe$_3$Al as received and thermally treated in de-aerated Hank´s solution at 37°C.
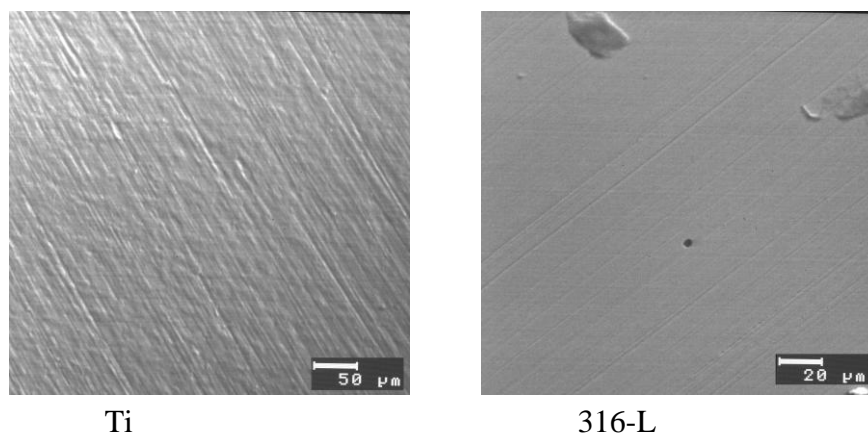
| Ti | 316-L |

Figure 11. SEM photographs of Ti and 316-L after cyclic polarization test in de-aerated Hank's solution at 37°C.

| Fe₃Al | Fe₃Al (TT) |

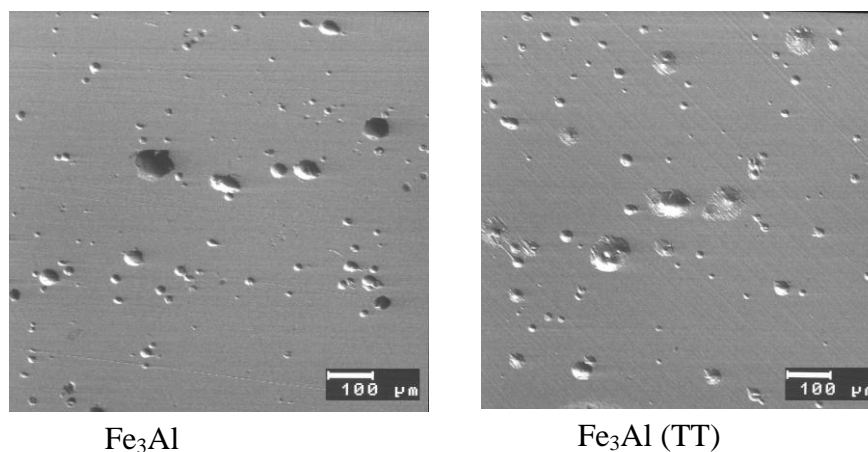Fe_3Al Fe_3Al (TT)

Figure 12. SEM photographs of Fe_3Al modified with Ni in the as cast and thermally treated conditions after cyclic polarization test in de-aerated Hank's solution at 37°C.

This value corresponds exactly to the area where the metastable pitting behavior indicated above started. This may be due because these authors in their study used a 316-L steel manufactured by them and in this paper a commercial alloy was utilized. Similar studies in acidic conditions (pH = 4) indicate that pitting potential is 100 mV [22], or 850 mV in tests at 18°C [25]. Surface observations made by SEM showed the presence of very small pits (figure 11).

The behavior shown by Fe_3Al, in as cast and thermally treated conditions, was similar. Thermal treatment only affects the corrosion potential of the material making it more active. Curves shows that both materials lack of a passive zone. This indicates an inability to build a stable protective oxide on its surface. Alloys of the same type and in similar experimental conditions show a stability zone allowing the formation of a protective oxide, but despite this, they also show a tendency to pitting corrosion [23]. Figure 12 shows the surface appearance of these materials after the test, which reveals the high density of pits formed on its surface.

Figure 13 shows the effect of Ni addition to Fe$_3$Al in as cast and thermal treated conditions. The as cast condition shows that Ni addition changed the corrosion potential of the base alloy, but the general behavior of alloys with Ni is similar to the behavior shown by the base alloy. Thermal treatment improved the corrosion behavior of Fe$_3$Al-3Ni and Fe$_3$Al-5Ni alloys. It is observed a trend to build a passive zone when Ni content is increased. This effect is clearest in the Fe$_3$Al-5Ni alloy, having a pitting potential of -170 mV, however, a protection potential during the reverse sweep was not detected. Although the Fe$_3$Al-3Ni alloy did not showed clearly a passive zone, it had a pitting potential to -200 mV.
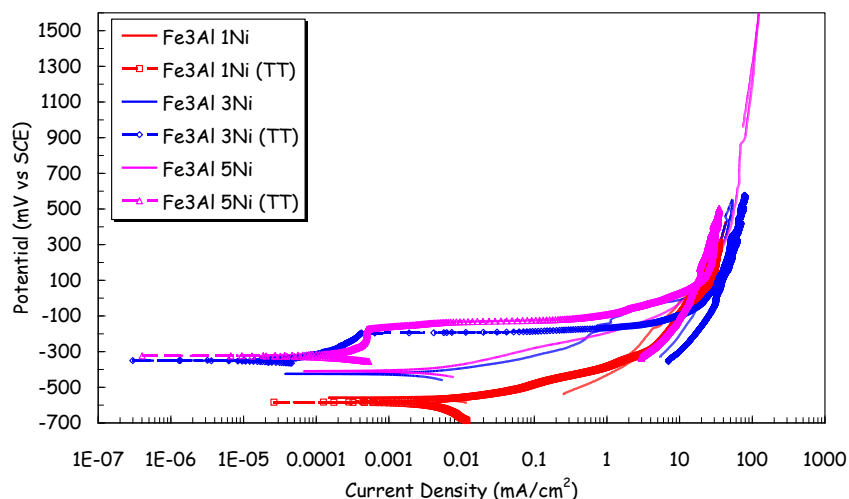

Figura 13. Cyclic polarization plots of Fe$_3$Al modified with Ni in as cast and thermally treated conditions in de-aerated Hank´s solution at 37°.

Figure 14 shows the surface aspects of these alloys after the tests. It is observed that the thermally treated alloys showed a lower pitting density compared to the cast alloys. The appearance of the surface attack showed by all intermetallic alloys is consistent with the morphology type reported for the pitting attack of this type of alloys in environments containing chlorides [8].

Frangini et al. [5] present a summary of the different cyclic polarization curves characteristics expected for materials susceptible to pitting and crevice corrosion. According to this classification, it can be state that Ti and 316-L behavior correspond to the typical response of materials susceptible to pitting corrosion. Behavior shown by all different intermetallic alloys tested corresponds to that of materials susceptible to crevice corrosion without showing a repassivation area. This behavior is due to the formation of contiguous pits whose growth and their coalescence manifested as crevice. Although Ni addition and thermal treatment increased the corrosion resistance of Fe$_3$Al, the corrosion resistance of the passive layer developed was not able to withstand in chloride-rich environments as it has been shown in other studies [15]. Additionally, it has been reported [16, 24] that Ni addition increases the probability of crevice corrosion in Hank´s solution.
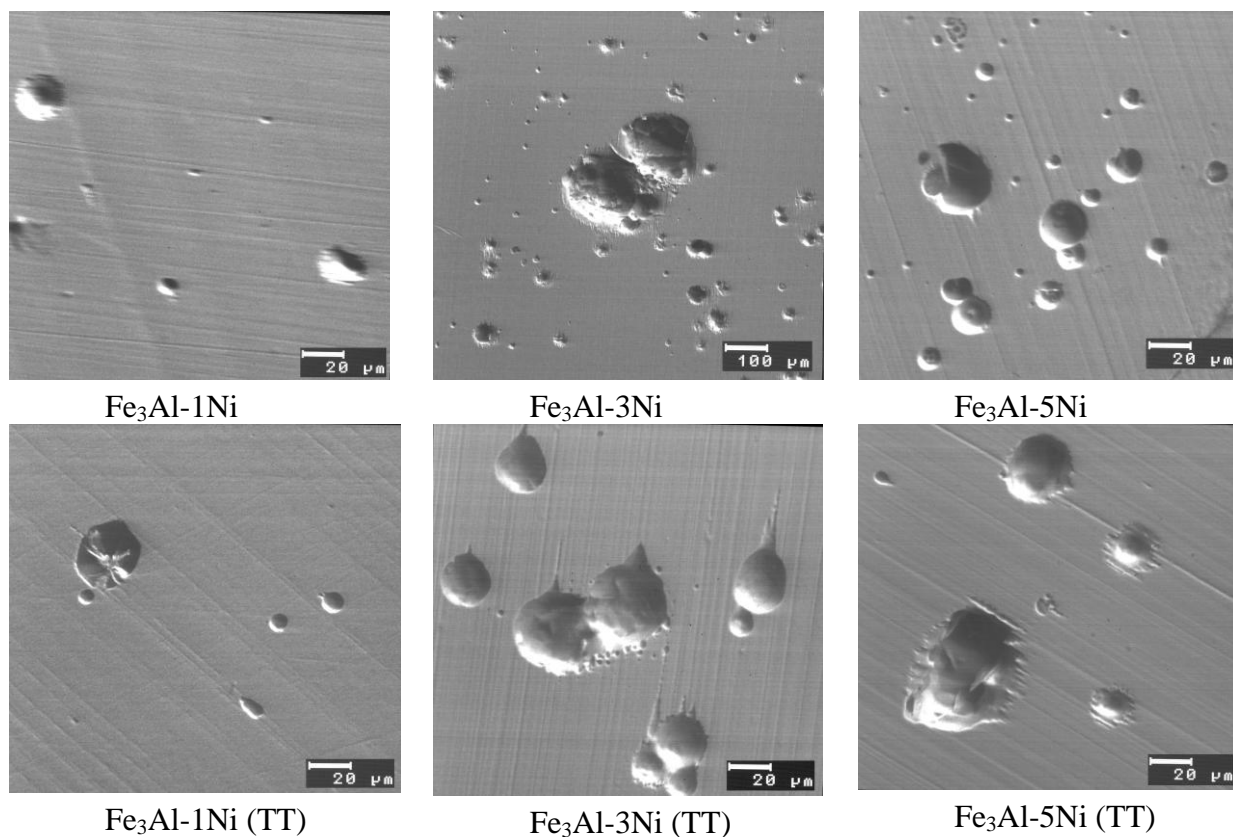
Figure 14. SEM photographs of Fe$_3$Al modified with Ni in the cast and thermally treated conditions after cyclic polarization test in de-aerated Hank's solution at 37°C.

4. CONCLUSIONS

The favorable effect of Ni addition to the Fe$_3$Al intermetallic for improving its corrosion resistance has been demonstrated. Heat-treated Fe$_3$Al with Ni addition further increase its corrosion resistance. However, pitting resistance of Fe$_3$Al intermetallic alloys compared to Ti and 316-L stainless steel showed a greater susceptibility to pitting corrosion. Among all materials, 316-L stainless steel and titanium were the materials with greater corrosion resistance in chloride-rich environments such as Hank´s solution.

Corrosion rates of Fe$_3$Al intermetallic with Ni additions can compare favorably with the corrosion rate of Titanium in Hank´s solution, but not with its localized corrosion resistance. So, if Fe$_3$Al with Ni addition are intended as a biomaterial, their localized corrosion resistance must be improved by alloying with suitable elements.

References

1. L.L. Hench, *Inorganic biomaterial, in Advances in chemistry series 245: Materials chemistry – an emerging discipline*, American Chemical Society, Washington DC (1985).
2. A.F. Von Recum, *Handbook of biomaterials evaluation,* Taylor & Francis Inc. Philadelphia (1999).
3. J. Lemons, H. Freese, *Metallic biomaterials for surgical implant devices. BONEZone*, Knowledge Enterprises, Inc. (2002)
4. H. Yang, K. Yang, B. Zhang, *Materials Letters* 61 (2007):1154.
5. S. Frangini, N. De Cristofaro, *Corros Sci* 45 (2003):2769.
6. P.F. Tortorelli, P.S. Bishop, *in Environmental Effects on Advanced Materials*, The Minerals, Metals and Materials Society, Warrendale, P.A., (1991).
7. P.F. Tortorelli, K. Natesan, *Mater Sci Eng* A258 (1998):115.
8. V.S. Rao, *Electrochimica Acta* 49 (2004):4533.
9. X. Cheng, S.G. Roscoe, *Biomaterials* 26 (2005):7350.
10. S. Tamilselvi, V. Raman, N. Rajendran, *Electrochimica Acta* 52 (2006):839.
11. S. Luiz de Assis, S. Wolynec, I. Costa, *Electrochimica Acta* 51 (2006):1815.
12. H. Yang, K. Yang, B. Zhang, *Materials Letters* 61 (2007):1154.
13. M. Salazar, A. Albiter, G. Rosas, R. Perez, *Mat. Sci. Eng.* 351A (2003):154.
14. I. Gurappa, *Materials Characterization* 49 (2002):73.
15. M.F. Lopez, M.L. Escudero, *Electrochem. Acta* 43 (1998):671.
16. K.M. Speck, A.C. Fraker, *J. Dent. Res*. 59 (1980):1590.
17. Daniel Rodríguez Rius, *PhD Thesis*, Universitat Politècnica de Catalunya, 1999.
18. R.J. Solar, *Corrosion resistance of titanium surgical implant alloys: a review*, ASTM STP 684, Baltimore (1979).
19. C. Fonseca, A. Traverse, A. Tadjeddine, M.C. Belo, *J. Electroanal. Chem.* 388 (1995):115.
20. J. Pan, D. Thierry, C. Leygraf, *Electrochimica Acta* 41(1996):1143.
21. F.J. Gil, M.P. Ginebra, A. Padrós, J.A Planell, *Revista Española Odontoestomatológica de Implantes*, 2 (1993):113.
22. A. Cakir, S. Tuncell, A. Aydin, Corros Sci 41(1999):1175.
23. M.C. Garcia-Alonso, M.F. Lopez, M.L. Escudero, J.L. Gonzalez-Carrasco, D.G. Morris, *Intermetallics* 7 (1999):185
24. F.T. Cheng, K.H. Lo, H.C. Man, *J. Alloys. Compounds* 437 (2007):322.
25. Eugénia Leitao, *PhD Thesis*, Universidad de Oporto, 1996.